doi:10.1016/j.ultrasmedbio.2003.11.007

● *Original Contribution*

TRACKING OF REGIONS-OF-INTEREST IN MYOCARDIAL CONTRAST ECHOCARDIOGRAPHY

Norberto Malpica,* Andres Santos,* Miguel Ángel Zuluaga,[†] María J. Ledesma,*
Esther Pérez,[‡] Miguel A. García-Fernández[‡] and Manuel Desco[†]

*Dpto. Ingeniería Electrónica, ETSI Telecomunicación, Universidad Politécnica de Madrid, Madrid, Spain;
[†]Laboratorio de Imagen, Medicina Experimental; and [‡]Laboratorio de Ecocardiografía, Departamento de
Cardiología, Hospital General Universitario Gregorio Marañón, Madrid, Spain

Abstract—Analysis of intramyocardial perfusion by contrast echocardiography provides quantitative parameters for the assessment of ischemic disease. This analysis can be achieved by applying an ultrasound (US) burst of high mechanical index to destroy contrast bubbles, measuring various myocardial refilling parameters from the time curves obtained from regions-of-interest (ROIs) within the myocardial wall. To obtain reliable intensity curves, the position of the ROIs must be tracked to compensate for the heart motion along the sequence. In this work, we studied the use of optical flow techniques for ROI repositioning. Two block-matching and one differential technique were evaluated for this purpose. Performance was measured by comparing the result of automatic tracking with results of ROI repositioning by a human expert. This evaluation was carried out on experimental data from animals as well as on sequences from clinical studies. Results are considered to be accurate enough for clinical purposes, and computation times may allow for a real-time processing if incorporated into a US scanner. (E-mail: desco@mce.hggm.es) © 2004 World Federation for Ultrasound in Medicine & Biology.

Key Words: **Perfusion, Quantitative analysis, Optical flow, Ischemia, Motion.**

INTRODUCTION

Analysis of the heart wall motion is a standard technique for studying myocardial viability (Fedele et al. 1998). In some cases, however, it is not sufficient to identify a pathologic region. For example, stunned myocardium is a postischemic dysfunction characterized by regions with motion abnormalities, but normal flow, that may recover in the following weeks. Myocardial contrast echocardiography (MCE), due to its ability to assess microvascular integrity, has been shown to provide markers of successful reperfusion of acute myocardial infarction (Vannan and Kuersten 2000). Viability of the myocardium is estimated by the degree of myocardial opacification following contrast injection. Absence of myocardial opacification after reperfusion has been associated with necrosis and failure to recover function (Ohmori et al. 2001).

A method for obtaining quantitative parameters consists of acquiring images during the myocardial refilling process after destroying the contrast microbubbles with an ultrasound (US) pulse of high energy (high mechanical index). It is, thus, possible to obtain not only steady-state region intensity, but also the wash-in curve showing the refilling of the region after the destruction of the microbubbles (Desco et al. 2001a; Masugata et al. 2001). In routine analysis, regions-of-interest (ROIs) are traced on the image and time-intensity curves are drawn from each of them (Tani et al. 2002). These time curves are adjusted to mathematical models, whose parameters provide quantitative information on the degree of reperfusion (Jayaweera et al. 1994). Images from a sequence and the time curves corresponding to two ROIs are shown in Fig. 1. The fitted exponential models are also shown. Notice the different degree of reperfusion of both regions.

Acquisition can be carried out in electrocardiogram (ECG)-triggered mode (images are synchronously obtained at the same point of the cardiac cycle), but a higher sampling rate may be achieved in continuous mode, in which images are obtained asynchronously at a constant frame rate. In this case, as the heart moves, a fixed ROI position does not represent the same structures

Address correspondence to: Dr. M. Desco, Medicina Experimental, Hospital General Universitario "Gregorio Marañón," Madrid E-28007 Spain. E-mail: desco@mce.hggm.es

along the cardiac cycle. Therefore, for accurate quantification, regions must be repositioned along the sequence. In previous works, registration based on cross-correlation has been used to align the images (Jayaweera et al. 1994). In these works, only end diastole short-axis views were used and complete images were aligned using rigid registration by cross-correlation. Recently, a nonrigid registration approach has also been used on two-chamber views (Noble et al. 2002). This study was based on sequences acquired in triggered mode, which ensures a small displacement along the sequence. In studies using real-time (continuous) acquisition mode, ROIs are usually realigned manually for quantification (Di Bello et al. 2002; Van Camp et al. 2003).

Optical flow computation has been and still is one of the major areas of research in computer vision. Optical flow techniques are generally classified into differential, matching, energy-based and phase-based methods. A comprehensive review of optical flow algorithms can be found in Barron et al. (1994). Although previous studies have shown that speckle motion does not represent perfectly tissue motion (Kallel et al. 1994), tracking methods are being widely applied in US. Tracking of time-domain speckle using optical flow offers an alternative to Doppler imaging to estimate tissue motion (Hein and O'Brien 1993). Time-domain methods have found applications in biomedical imaging, including the assessment of myocardial deformation (Mailloux et al. 1989). Baraldi et al. (1996) compared several differential techniques on synthetic echo images. More recently, optical flow techniques have been used in conventional echocardiography to guide segmentation algorithms (Giachetti 1998). In Yeung et al. (1998a), a multilevel speckle-tracking algorithm was presented and evaluated using a phantom.

The aim of our work was to implement and evaluate local block-matching algorithms as a tool to track ROIs along the sequence. We also evaluate the efficiency of local tracking algorithms that should provide faster re-positioning than global morphing schemes, such as grid-base (Yeung et al. 1998b) or registration (Noble et al.

2002) approaches. Two block-matching techniques and one differential one were compared, both on experimental images obtained from pigs and on clinical sequences from patients. To the best of our knowledge, there are no published works about region tracking in contrast echocardiography.

MATERIALS AND METHODS

Block-matching techniques

Window-matching or correlation-based techniques are the most widely applied techniques to compute the optical flow from an image sequence (Giachetti 2000). They are based on the analysis of the grey-level pattern around the point-of-interest and on the search for the most similar pattern in the following image. The basic implicit assumption is that the grey-level pattern remains approximately constant between successive frames and that local texture contains sufficient unambiguous information. Correlation-based techniques have been used for motion detection in conventional US (Giachetti 1998). A thorough review of these methods can be found in Giachetti (2000).

Matching-based tracking. Let I_1 and I_2 be two images corresponding to two neighbor frames. Having defined a window $W(\vec{x})$ around the point $\vec{x}$ in image I_1, a similar window $W'(\vec{x} + \vec{d})$ in image I_2 is considered, shifted by an integer number of pixels in a search space S. The motion vector (*i.e.,* the estimated image displacement) is obtained as the shift corresponding to the minimum value of a distance function (or maximum of a correlation measure) between the intensity patterns in the two corresponding windows:

$$\text{dist} = f(W, W'(\vec{d})). \tag{1}$$

We have evaluated two different distance functions, namely the normalized sum-of-squared differences (NSSD):

$$NSSD(\vec{x}, \vec{d}) = \frac{\displaystyle\sum_{i,j=-N/2}^{N/2} (I_1(x+i, y+j) - I_2(x+i+d_x, y+j+d_y))^2}{\displaystyle\sum_{i,j=-N/2}^{N/2} (I_1(x+i, y+j) \cdot \sum_{i,j=-N/2}^{N/2} (I_2(x+i+d_x, y+j+d_y)} \tag{2}$$

positioning than global morphing schemes, such as grid-base (Yeung et al. 1998b) or registration (Noble et al.

and the zero-mean normalized cross-correlation (Giachetti 2000):
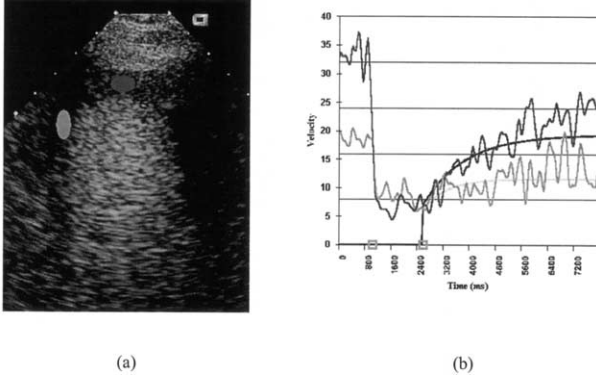
(a)   (b)

Fig. 1. (a) Image showing two user-defined ROIs, (b) time-intensity curves and fitted exponential models corresponding to the ROIs.

The contribution of each vector was weighted by the confidence factor $Q(\vec{x})$ of its *NSSD* computation.

Singh's algorithm. More complex algorithms may allow for subpixel accuracy by introducing stronger smoothness constraints on the motion. We have implemented Singh's algorithm (Singh 1990), which computes motion using three consecutive images, $im(-1)$, $im(0)$, $im(1)$, by minimizing the distance:

$$NSSD_3(\vec{x},\vec{d},im(-1),im(0),im(1)) =$$
$$= NSSD(\vec{x},\vec{d},im(-1),im(0))$$
$$+ NSSD(\vec{x},\vec{d},im(0),im(1)), \quad (5)$$

$$ZNCC(\vec{x},\vec{d}) = \frac{\displaystyle\sum_{i,j=-N/2}^{N/2} (I_1(x+i,y+j) - \bar{I}_1)(I_2(x+i+d_x,y+j+d_y) - \bar{I}_2)}{\displaystyle\sum_{i,j=-N/2}^{N/2} (I_1(x+i,y+j) \cdot \sum_{i,j=-N/2}^{N/2} (I_2(x+i+d_x,y+j+d_y)}, \quad (3)$$

where $\bar{I}_i$ is the mean grey level of image I in the correlation kernel.

As a measure of confidence, we use the ratio of the minimum value of the *NSSD* to the average distance in the search space $S(\vec{x})$:

$$Q(\vec{x}) = 1 - \frac{min_{\vec{d}\in S}NSSD(\vec{x},\vec{d})}{\bar{N}SSD}. \quad (4)$$

A value of Q close to 1 ensures a good correlation.

In all the experiments, a search region of 25×25 pixels and a correlation neighborhood of 35×35 were used.

Image subsampling. To reduce computing time, images were subsampled by a factor of two before applying correlation. A separable cubic B-spline filter (Pratt 1991) was applied to the images before subsampling to avoid aliasing. After checking that subsampling did not degrade performance, all block-matching algorithms included this step.

Spatial averaging. The shape of the ROI was fixed throughout the sequence. Only one global motion value was computed for the whole region. Assuming smoothness of neighboring motion vectors, we computed motion vectors for four evenly spaced points within the region and averaged the global motion vector from them.

where *NSSD* for two frames is defined in eqn (2).

A weight function is computed from the *NSSD* values:

$$R(\vec{x},\vec{d}) = e^{-k(\vec{x})NSSD(\vec{x}\vec{d})}, \quad (6)$$

where

$$k(\vec{x}) = -\ln(0.95)/min(NSSD_3(\vec{x},\vec{d},im(-1),$$
$$im(0),im(1)). \quad (7)$$

Subpixel displacement is then obtained as:

$$u(\vec{x}) = \frac{\sum R(\vec{x},\vec{d})d_x}{\sum R(\vec{d})}, \quad v(\vec{x}) = \frac{\sum R(\vec{x},\vec{d})d_y}{\sum R(\vec{d})}. \quad (8)$$

Differential techniques

Differential techniques compute motion from the spatiotemporal derivatives of the image intensity. Let $I(x,t)$ be the image intensity pattern at location x and time t and $m = (u(x),v(x))$ the motion field, where u and w represent the two velocity components. Differential techniques are based on the assumption that the image intensity pattern is constant along time:

$$\frac{dI(x,t)}{dt} = 0, \qquad (9)$$

Equation (9), referred to as the constant brightness equation, can be written as follows:

$$\nabla I(x,t) \cdot m + I_t(x,t) = 0 \qquad (10)$$

where ∇I denotes spatial image gradient and I_t denotes derivative with respect to t. Equation (10) is known as the gradient constraint equation.

We have implemented the algorithm proposed by Lucas and Kanade (1981) because it was the one with best results (both quantitative and subjective) in the comparisons presented by Barron et al. (1994) on natural scene sequences and by Baraldi et al. (1996) on synthesized US images. It is based on a weighted least squares (LS) fit of local first-order constraints in each small spatial neighborhood N, by minimizing:

$$\sum_{x \epsilon N} W^2(x)[\nabla I(x,t) \cdot m + I_t(x,t)]^2, \qquad (11)$$

where $W(x)$ denotes a window function that gives more influence to points at the center of the neighborhood than to those at the periphery. The solution to eqn (11) is given by:

$$A^T W^2 A m = A^T W^2 b \qquad (12)$$

where, for n points, x_i, ϵ N at a single time t,

$$A = [\nabla I(x_1), \ldots , \nabla I(x_n)] \qquad (13)$$

$$W = diag[W(x_1), \ldots , W(x_n)] \qquad (14)$$

$$b = -(I_t(x_1), \ldots , I_t(x_n))^T. \qquad (15)$$

To capture large displacements without a major increase in computational load, we adopted a multiscale scheme using a four-level Gaussian pyramid. The displacement was first computed at the lowest resolution. The algorithm was then applied at each level, starting from the displacements obtained in the previous level. Before computing velocities, images were smoothed with a Gaussian filter with an SD of 1.5 pixels. Ten iterations of the algorithm were applied to achieve convergence. An example of velocity vectors of nine points in an ROI is shown in Fig. 2.

Validation

Validation of optical-flow algorithms is usually performed using synthetized phantom sequences with a
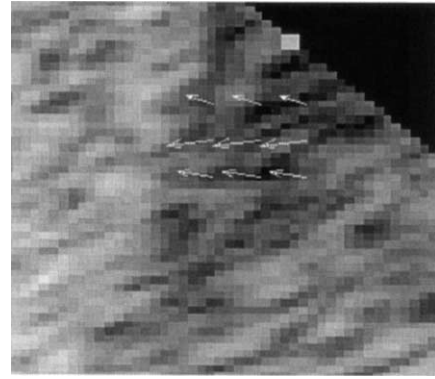

Fig. 2. Displacement vectors computed for nine points using the Lucas–Kanade approach.

known displacement (Baraldi et al. 1996). A realistic simulation of perfusion echocardiography and, particularly, the effect of the contrast media, is not an easy task and has been previously done using only very simple models (Fetics et al. 2001). In this work, evaluation was carried out from a practical point of view, by considering the repositioning by an expert as the "gold standard."

Five image sequences were used to evaluate the algorithms. Two of them were experimental studies obtained from open-chest pigs during surgery. The other three sequences were two-chamber views obtained from three different patients. Each sequence consisted of 40 frames, spanning approximately four cycles.

Experimental images obtained in animals were short-axis views from open-chest anesthetized pigs, using Sonovue® as echo-enhancer. Temporal resolution was 75 ms; pixel size was 0.3 mm. The transducer in this case was situated directly over the heart surface, producing images with higher contrast and well-defined myocardial borders, where myocardial refilling is better observed. Images obtained from pigs are part of an experimental protocol designed to test the validity of perfusion parameters with acute ischemia models. In this protocol, we acquired both basal images and images with a flow-limiting stenosis produced by reducing left anterior descending artery (LAD) flow by 50% of the baseline value. The latter were used for the evaluation because they include segments with different degrees of perfusion and wall motion. All aspects of animal handling and surgery were in accordance with the "European convention for the protection of vertebrate animals used for experimental and other scientific purposes" and with the local government regulations.

In patients, images were acquired with coherent contrast imaging (CCI), a single pulse cancellation method on an Acuson Sequoia (Acuson-Siemens, Mountainview, CA, USA) scanner. Images were acquired with a 3-MHz transducer in real-time (75 ms between frames)
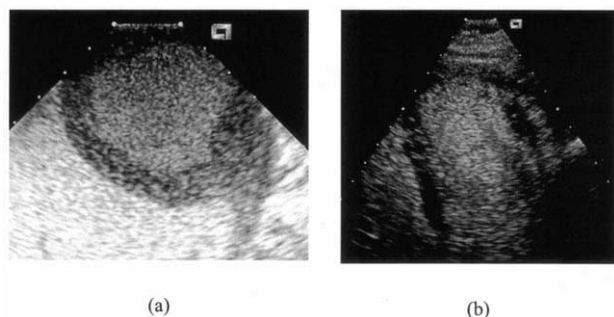
Fig. 3. (a) Short-axis view of an open-chest swine heart. (b) Two-chamber view of a patient heart.

during a continuous infusion of Sonovue® contrast agent; pixel size was 0.2 mm. After three cardiac cycles of homogeneous myocardial perfusion, microbubbles were destroyed with a pulse of high mechanical index (MI) (1.5) during three cardiac cycles and images of the replenishment phase were acquired with low MI (0.1 to 0.2).

In both experimental and clinical studies, ROIs must be tracked along the sequence to obtain time-intensity curves. Figure 3 shows representative frames of experimental and clinical sequences.

To evaluate the algorithm performance, three ROIs were placed in each sequence and automatic tracking was carried out using each of the tracking methods, in a supervised fashion. After automatic repositioning in each frame, the observer could either accept the result or manually change the position of the ROI. Two independent observers supervised the process on all the test sequences and the number of corrections required was recorded. As a reference measure, the users were asked to align manually the ROIs when required in every sequence, recording the number of frames where the user actually shifted the ROI. The number of corrections on all sequences and ROIs without applying any automatic tracking were also recorded and used as a reference measure. The ROIs were placed on different segments of the myocardium to take into account different degrees of motion and image quality. Interobserver differences were measured using the method proposed by Bland and Altman (1986). The mean and SD of the differences on all the sequences were computed. Performance of the different algorithms was measured by computing the mean and SD of the number of corrections by both observers for all of the sequences.

Because variables are not normally distributed, differences in performance among methods were evaluated using nonparametric analysis of variance using a Kruskal–Wallis test (Sokal and Rohlf 1995). *Post hoc*

comparisons were carried out by means of a Tukey honest significance difference (HSD) test, accepting a significance threshold of $p < 0.01$ to consider groups as different.

RESULTS

Figure 4 shows an example of several frames with ROIs repositioned automatically using the Lucas–Kanade algorithm.

Interobserver variability was measured by comparing the total number of frames corrected by each observer in all the sequences. A mean difference of 0.57% with an SD of the difference of 4.47% was obtained. Because the difference between observers was so low, validation results are presented using a merged set of measures from both users. Table 1 presents the results of the evaluation, showing the mean and SDs of the percentage of correct frames obtained with each of the algorithms on experimental and on clinical sequences. Figure 5 shows the results merged for all sequences.

The statistical analysis was applied considering all the sequences together. As a result of the Kruskal–Wallis test with *post hoc* comparisons, all the methods were demonstrated to perform significantly better ($p < 0.01$) than manual repositioning. Among these methods, the Lucas–Kanade algorithm was significantly better than the rest ($p < 0.01$). Among block-matching methods, differences were not significant. Using *NSSD* as distance yielded better results than *ZNCC*. Singh's algorithm improved the result of two-frame block-matching methods, at the expense of an increase in computing time.

Computation time for all the algorithms was short. The slowest is Lucas–Kanade, which took 0.5 s per frame on a Pentium IV PC. Automatic tracking methods have been included in an echocardiography quantification platform (Desco et al. 2001a, 2001b) that is currently used routinely for research in our hospital (Perez et al. 2001).

DISCUSSION

Results obtained with all the tracking methods were found to be significantly better than with manual tracking. The best results were achieved with the differential method, with similar computing times.

As expected, results obtained on the experimental sequences were better than those with patient data, due to the lower amount of noise present on these images. The effect of induced ischemia can be observed in the black nonperfused area of the myocardium in Fig. 4. One of the ROIs was placed on that region, with decreased motion, which could explain the better results obtained for that region. In US imaging, speckle actually varies with depth. Our evaluation included regions at different
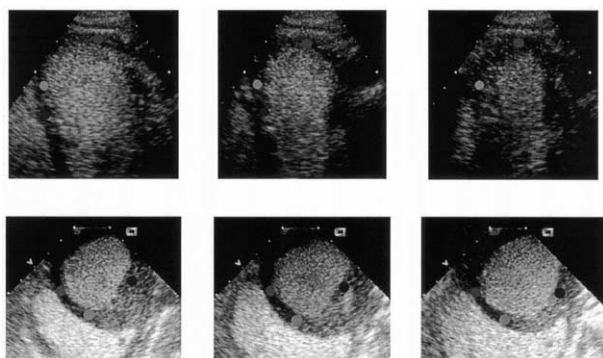
Fig. 4. Results of ROI tracking using the differential technique on (top) patient images and (bottom) open-chest animal images.

Fig. 5. Box plot of the percentages of correct frames obtained with each of the methods. 1 = no tracking, 2 = block-matching with *ZNCC* distance, 3 = block-matching with *NSSD* distance, 4 = Lucas–Kanade, and 5 = Singh.

depths in the myocardium that did not show differences in performance.

The use of three frames in Singh's algorithm improved the results obtained with the standard correlation technique, but is computationally more demanding and differences were not significant.

Two parameters were required in the algorithms, namely the size of the search region and the size of the correlation kernel. The first one depends on the maximum excursion expected between neighbor frames, which, in turn, depends on the acquisition frame rate. Pyramidal implementations allow detecting large interframe displacements with a small computational effort. The size of the correlation window depends on the speckle pattern; it must be large enough to capture tissue texture, although too large windows may hinder resolution of optical flow. The aim of our application was to move individual ROIs, so optical flow resolution was not an issue and the correlation windows used were large enough to assure a reliable result.

In our experiments, the frame rate used was high enough to assure a low interframe replenishment of contrast, being reasonable to assume approximately constant intensity between frames. Optical flow methods that take into account brightness variations along time have been recently proposed (Haussecker and Fleet 2001) but they require a precise mathematical description of the brightness variation model. In the case of contrast echocardi-
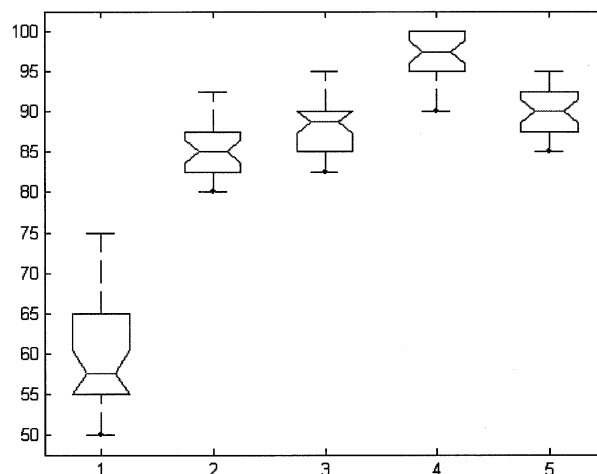
ography, the reperfusion function may differ between patients, as well as between different segments in an image.

No prior information about expected motion was included in any of the algorithms. Incorporating *a priori* knowledge of heart motion or using results from previous heart cycles to correct motion vectors could further improve our results.

During evaluation, we observed that, when using a totally manual repositioning tool, a typical user only moves the ROI every few frames, when a misplacement is clearly visible, but the automatic algorithm computes a displacement in all frames, thus achieving a better resolution. This leads us to presume that the automatic method could even be more exact, although this cannot be affirmed based on the evaluation performed. Further studies, maybe with phantoms, would be needed.

A limitation of the study is that size and shape of the regions was kept constant during the whole sequence because this is the way studies are performed in clinical practice. ROIs are used only to sample the grey level in a myocardial region; thus, it is not necessary to change their shape along time. In our approach, region tracking

Table 1. Mean number of correct displacements (percentages) and SD for each of the algorithms

	Manual positioning	Matching-*ZNCC*	Matching-*NSSD*	Lucas–Kanade	Singh
Group I sequences	65.2 ± 5.4	86.6 ± 4.2	88.6 ± 3.5	97.7 ± 2.4	88.1 ± 3.1
Group II sequences	56.3 ± 3.5	85.4 ± 3.4	89.1 ± 3.4	95.0 ± 2.8	90.0 ± 3.0

Group I sequences were obtained from open-chest pigs; group II sequences are clinical sequences obtained from patients.

is independent of region shape. Computing the displacement vector for all the points in the region could be the basis for an adaptive ROI analysis, at the expense of computing time.

Another limitation is that conventional 2-D US imaging can only capture in-plane motion, although heart motion is 3-D and interplane motion could modify speckle patterns. This is a limitation inherent to all methods that work on bidimensional imaging and will be easier to face when 3-D echocardiography becomes a tool in routine clinical use. Some initial experimental works have already been presented (Camarano et al. 2002).

CONCLUSIONS

We have implemented and evaluated three optical flow algorithms for ROI tracking in contrast echocardiography sequences. Results are encouraging because algorithms have been shown to be accurate and fast enough for real-time processing. The differential method yielded better results than block-matching methods with similar execution times. We have designed an interactive tracking tool, already included in a contrast quantification software currently used for clinical research in several hospitals.

REFERENCES

Baraldi P, Sarti A, Lamberti C, Prandini A, Sgallari F. Evaluation of differential optical flow techniques on synthesized echo images. IEEE Trans Biomed Eng 1996;43:259–272.

Barron JL, Fleet DJ, Beauchemin SS. Performance of optical flow techniques. Int J Comput Vision 1994;12:43–77.

Bland JM, Altman DG. Statistical methods for assessing agreement between two methods of clinical measurement. Lancet 1986;1:307–310.

Camarano G, Jones M, Freidlin RZ, Panza JA. Quantitative assessment of left ventricular perfusion defects using real-time three-dimensional myocardial contrast echocardiography. J Am Soc Echocardiogr 2002;15:206–213.

Desco M, Ledesma-Carbayo MJ, Santos A, et al. Myocardial perfusion with contrast echocardiography. In: Insana MF, ed. Medical imaging 2001: Ultrasonic imaging and signal processing. Proc. of SPIE Vol. 4325. San Diego, 2001a:514–522.

Desco M, Ledesma-Carbayo MJ, Santos A, et al. Coherent contrast imaging quantification for myocardial perfusion assessment. J Am Coll Cardiol 2001b;37:495A.

Di Bello V, Pedrinelli R, Giorgi D, et al. Coronary microcirculation in essential hypertension: A quantitative myocardial contrast echocardiographic approach. Eur J Echocardiogr 2002;3:117–127.

Fedele F, Trambaiolo P, Magni G, De Castro S, Cacciotti L. New modalities of regional and global left ventricular function analysis: State of the art. Am J Cardiol 1998;81:49G–57G.

Fetics BJ, Wong EY, Murabayashi T, et al. Enhancement of contrast echocardiography by image variability analysis. IEEE Trans Med Imaging 2001;20:1123–1130.

Giachetti A. On-line analysis of echocardiographic image sequences. Med Image Anal 1998;2:261–284.

Giachetti A. Matching techniques to compute image motion. Image Vision Comput 2000;18:247–260.

Haussecker HW, Fleet DJ. Computing optical flow with physical models of brightness variation. IEEE Trans Pattern Anal Machine Intell 2001;23:661–673.

Hein IA, O'Brien WD. Current time-domain methods for assessing tissue motion by analysis from reflected ultrasound echoes—A review. IEEE Trans Ultrason Ferroelec Freq Control 1993;40:84–102.

Jayaweera AR, Matthew TL, Sklenar J, et al. Method for the quantification of myocardial perfusion during myocardial contrast two-dimensional echocardiography. J Am Soc Echocardiogr 1994;3:91–98.

Kallel F, Bertrand M, Meunier J. Speckle motion artifact under tissue rotation. IEEE Trans Ultrason Ferroelec Freq Control 1994;41:105–122.

Lucas B, Kanade T. An iterative image registration technique with an application to stereo vision. In: Proceedings DARPA IU Workshop. 1981:121–130.

Mailloux GE, Langlois F, Simard PY, Bertrand M. Restoration of the velocity field of the heart from two dimensional echocardiograms. IEEE Trans Med Imaging 1989;8:143–153.

Masugata H, Peters B, Lafitte S, et al. Quantitative assessment of myocardial perfusion during graded coronary stenosis by real-time myocardial contrast echo refilling curves. J Am Coll Cardiol 2001;37:262–269.

Noble JA, Dawson D, Lindner J, Sklenar J, Kaul S. Automated non-rigid alignment of clinical myocardial contrast echocardiography image sequences: Comparison with manual alignment. Ultrasound Med Biol 2002;28:115–123.

Ohmori K, Cotter B, Leistad E, et al. Assessment of myocardial postreperfusion viability by intravenous myocardial contrast echocardiography: Analysis of the intensity and texture of opacification. Circulation 2001;103:2021–2027.

Perez E, Garcia-Fernandez MA, Desco M, et al. Real time myocardial contrast quantification in the right ventricle: Comparison with left ventricle myocardial perfusion evaluated with a new contrast agent. Eur J Echocardiogr 2001;2:S86.

Pratt WK. Digital image processing. New York: Wiley, 1991.

Singh A, Allen P. Image-flow computation: An estimation-theoretic framework and a unified perspective. Computer Vision, Graphics and Image Processing 1992;56:152–177.

Sokal RR, Rohlf FJ. Biometry. New York: W. H. Freeman, 1995.

Tani T, Tanabe K, Ono M, et al. Quantitative assessment of harmonic power Doppler myocardial perfusion imaging with intravenous Levovist™ in patients with myocardial infarction: Comparison with myocardial viability evaluated by thallium-201 single-photon emission computed tomography and coronary flow reserve. Eur J Echocardiogr 2002;3:287–297.

Van Camp G, Ay T, Pasquet A, et al. Quantification of myocardial blood flow and assessment of its transmural distribution with real-time power modulation myocardial contrast echocardiography. J Am Soc Echocardiogr 2003;16:263–270.

Vannan MA, Kuersten B. Imaging techniques for myocardial contrast echocardiography. Eur J Echocardiogr 2000;1:224–226.

Yeung F, Levinson SF, Parker KJ. Multilevel and motion model-based ultrasonic speckle tracking algorithms. Ultrasound Med Biol 1998a;24:427–441.

Yeung F, Levinson SF, Fu D, Parker KJ. Feature-adaptive motion tracking of ultrasound image sequences using a deformable mesh. IEEE Trans Med Imaging 1998b;17:945–956.